

Radiating Properties of Dielectric Covered Apertures

By ELLIOTT R. NAGELBERG

(Manuscript received May 21, 1968)

This paper studies the effect of a dielectric sheath on the far-zone radiation characteristics of an aperture bounded by a perfectly conducting ground plane. An examination of the appropriate Green's function predicts a significant broadening of the radiation pattern in a narrow band centered about that frequency at which a surface wave would begin to propagate along a grounded dielectric slab with the same thickness and permittivity as the sheath. The differences between this phenomenon and what is commonly referred to as a surface wave are discussed. Experimental results are then presented for the broadside and end-fire (perpendicular to the aperture) radiation by a waveguide aperture, from which it is found that the theory does predict the essential character of the observations.

I. INTRODUCTION

In designing phased arrays for radar and other types of communication systems, it is generally necessary to provide some degree of environmental protection. One configuration which suggests itself is the flush-mounted "radome" (Fig. 1), made of a suitable refractory ceramic such as beryllia, alumina, or boron nitride. However, since these materials typically have relative dielectric constants greater than unity, such a covering sheath can be expected to influence the electrical performance of the antenna and hence of the system to which it belongs. The two antenna characteristics of greatest interest are: (i) the individual element input impedance and (ii) the radiation pattern corresponding to a given aperture illumination.

The effects of a covering sheath on the input characteristics of infinite rectangular waveguide arrays have been discussed by Galindo and Wu, using a technique of spectral analysis.¹ Although the radiation pattern of a single element in an array environment can also be obtained as a by-product of this analysis, it is still useful to study

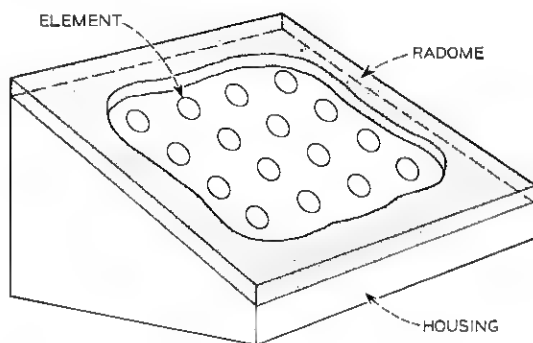


Fig. 1 — Segment of a phased array antenna with protective radome.

a single isolated element, particularly in order to distinguish characteristics which are associated with the element itself from those attributable to the periodicity of the structure. If the individual elements are identical, then the far-field radiation pattern of the total array can be represented as the product of the element pattern (in the array environment so that mutual coupling effects are included) and the array factor, which depends on the periodicity of the aperture and the overall amplitude and phase taper. The sheath does not alter this separability feature and can be regarded as affecting only the element pattern.

As an example, we have chosen to study the radiating properties of a single continuous aperture in a ground plane, covered by a dielectric slab of known thickness and permittivity. A study of the appropriate Green's function shows that the principal effect of the sheath is a significant broadening of the radiation pattern, over a narrow band centered about the frequency at which a surface wave would begin to propagate along the grounded dielectric sheath alone. (It follows that under matched conditions there must also be a dip in the broadside radiation, as required by energy conservation.) The result of this broadening is to produce a sharp increase in the power radiated near the end-fire direction. It should be pointed out, however, that despite the mathematical connection, this radiation differs from a "surface wave"² in two respects: (i) It belongs to the continuous spectrum of the radiation field and thus should be regarded physically as a distortion of the far-zone pattern rather than a separate mode of propagation; it thus exhibits the characteristic inverse power law variation with distance from the aperture. (ii) The end-fire signal amplitude is roughly symmetrical about the surface wave cut-

off frequency and thus does not itself exhibit a cut-off characteristic.

First we outline the formal solution to the boundary value problem, which is carried out by a Fourier transform analysis. Then we obtain the far-zone field by a saddle point approximation to the inversion integral, from which the broadening is clearly shown by direct evaluation. Finally, we discuss the associated experimental work and present results which serve to corroborate the theoretical analysis. We use rationalized MKS units and the (suppressed) harmonic time dependence $e^{-i\omega t}$ throughout.

There is a mathematical question regarding the validity of the saddle point approximation under the conditions $\theta \simeq \pi/2$ and $k_0 a = (k_0 a)_n$. For this combination of parameters, the denominator of the function $F(\alpha)$ in equation (11) vanishes at the saddle point. Notice that the presence of the $\cos \alpha$ factor causes the integrand to be finite under these circumstances so that the procedure is still valid. Another point of view is that when the saddle point and "pole" coalesce, the residue vanishes and with it the necessary correction term to the steepest descent formula (see Ref. 3, p. 503).

II. THEORETICAL ANALYSIS

The problem is to determine the far-zone radiating properties of an aperture covered by a dielectric sheath, as shown in Fig. 2. It is assumed that the electric field is in the y direction and that all quantities are independent of y . In addition to its mathematical simplicity,

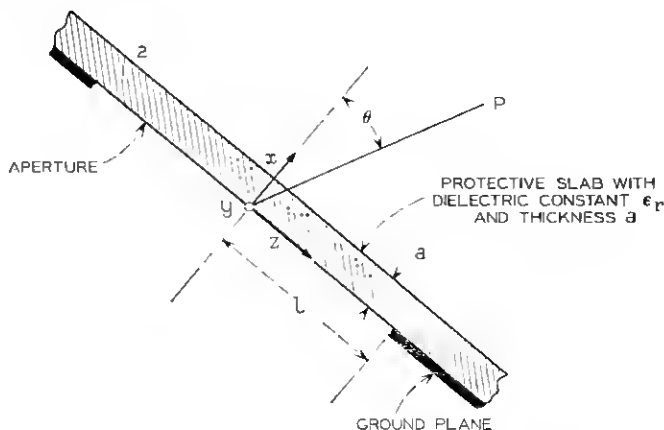


Fig. 2—Aperture of width $2l$ bounded by ground plane and covered by protective slab of thickness a and dielectric constant ϵ_r .

off frequency and thus does not itself exhibit a cut-off characteristic.

First we outline the formal solution to the boundary value problem, which is carried out by a Fourier transform analysis. Then we obtain the far-zone field by a saddle point approximation to the inversion integral, from which the broadening is clearly shown by direct evaluation. Finally, we discuss the associated experimental work and present results which serve to corroborate the theoretical analysis. We use rationalized MKS units and the (suppressed) harmonic time dependence $e^{-i\omega t}$ throughout.

There is a mathematical question regarding the validity of the saddle point approximation under the conditions $\theta \simeq \pi/2$ and $k_0 a = (k_0 a)_n$. For this combination of parameters, the denominator of the function $F(\alpha)$ in equation (11) vanishes at the saddle point. Notice that the presence of the $\cos \alpha$ factor causes the integrand to be finite under these circumstances so that the procedure is still valid. Another point of view is that when the saddle point and "pole" coalesce, the residue vanishes and with it the necessary correction term to the steepest descent formula (see Ref. 3, p. 503).

II. THEORETICAL ANALYSIS

The problem is to determine the far-zone radiating properties of an aperture covered by a dielectric sheath, as shown in Fig. 2. It is assumed that the electric field is in the y direction and that all quantities are independent of y . In addition to its mathematical simplicity,

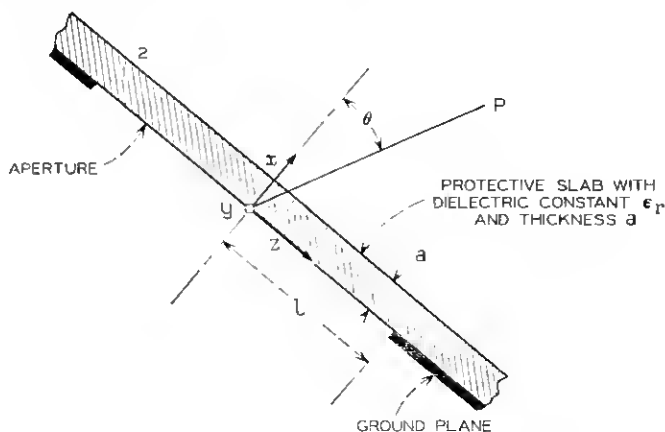


Fig. 2—Aperture of width $2l$ bounded by ground plane and covered by protective slab of thickness a and dielectric constant ϵ_r .

this two-dimensional situation can be realized experimentally by erecting parallel conducting planes perpendicular to the electric field.

Using a plane wave (Fourier) spectrum representation of the fields, E_y is given in terms of the transform pair

$$E_y(x, z) = \frac{1}{2\pi} \int_{h=-\infty}^{+\infty} G(h, z) e^{ihx} dh \quad (1)$$

$$G(h, x) = \int_{z=-\infty}^{+\infty} E_y(x, z) e^{-ihz} dz \quad (2)$$

where h , the transform variable, denotes the z -directed propagation constant of the particular plane wave component.

The function $G(h, x)$ thus satisfies the one-dimensional wave equation

$$\frac{d^2 G(h, x)}{dx^2} + \beta^2 G(h, x) = 0 \quad (3)$$

where

$$\beta = (k^2 - h^2)^{1/2} \text{ inside the sheath}$$

$$\beta = \beta_0 = (k_0^2 - h^2)^{1/2} \text{ outside the sheath,} \quad (4)$$

k or k_0 being the respective wave number. The proper Riemann surface, shown in Fig. 3, defines the square root such that

$$\beta = +(k^2 - h^2)^{1/2} \text{ } h \text{ real, } |h| < k \quad (5a)$$

$$\beta = +i(h^2 - k^2)^{1/2} \text{ } h \text{ real, } |h| > k. \quad (5b)$$

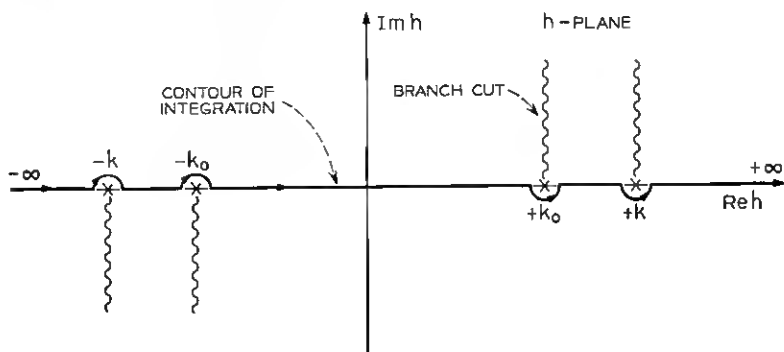


Fig. 3 — Definition of proper Riemann surface for evaluation of $\beta_0 = (k_0^2 - h^2)^{1/2}$ and $\beta = (k^2 - h^2)^{1/2}$.

Conditions given by equations (5a) and (5b) are a result of the physical requirements that: (i) waves radiated far from the aperture travel in the $+x$ direction and (ii) slow waves propagating in the $\pm z$ direction decrease exponentially in amplitude with distance from the sheath.

The boundary conditions are that

$$G(h, 0) = G_0(h) \quad (6a)$$

$$G, \frac{\partial G}{\partial x} \text{ continuous at } x = a \quad (6b)$$

where $G_0(h)$ is the Fourier transform of the aperture illumination.

The principal interest is in the field in region 2, outside the sheath, whose transform function is denoted by

$$G_2(h, x) = A(h)e^{i\beta_0 x}. \quad (7a)$$

In a similar manner we represent the field in region 1, inside the sheath as,

$$G_1(h, x) = B(h)e^{i\beta x} + C(h)e^{-i\beta x} \quad (7b)$$

and by direct substitution into (6) we find that

$$A(h) = \frac{G_0(h)e^{-i\beta_0 a}}{\cos \beta a - i \frac{\beta_0}{\beta} \sin \beta a}. \quad (8)$$

This leads directly to the expression for E_y

$$E_y(x, z) = \frac{1}{2\pi} \int_{-\infty}^{+\infty} \frac{G_0(h)e^{-i\beta_0 a}}{\cos \beta a - i \frac{\beta_0}{\beta} \sin \beta a} e^{i\beta_0 x} e^{i h z} dh \quad (9)$$

The determination of the far-zone radiation pattern from integral representations of the form given in equation 9 generally proceeds by saddle point integration. We first transform into the polar coordinates r, θ shown in Fig. 2, which are related to x, z by

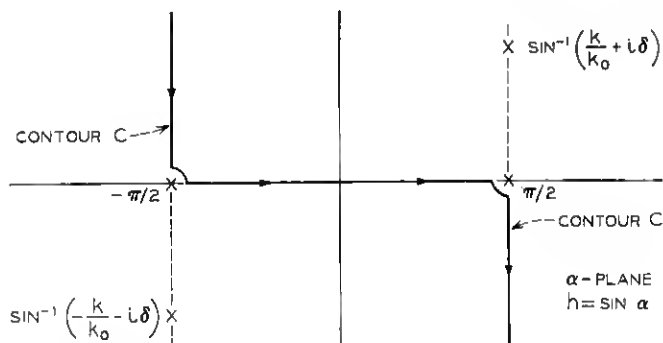
$$x = r \cos \theta \quad (10)$$

$$z = r \sin \theta.$$

Next, using the transformation $h = k_0 \sin \alpha$, we find that equation 9 can be written in the form

$$E_y(r, \theta) = \frac{1}{2\pi} \int_C F(\alpha) e^{i k_0 r \cos(\alpha - \theta)} \cos \alpha d\alpha \quad (11)$$

where the new contour is that given in Fig. 4. Notice also that in transforming from the h - to the α -plane, the integral is independent

Fig. 4—Transformation $h = \sin \alpha$ showing new contour.

of the sign of the square root and hence the branch cuts disappear. In order to compute the far-field we let $k_0 r \rightarrow \infty$ and use the saddle point method to determine an asymptotic formula for the integral.³ For purposes of finding the radiation pattern only, it is sufficient to observe that the saddle point occurs at $\alpha = \theta$ and that the *angular variation* of the field can therefore be specified in terms of the (unnormalized) function

$$G(\theta) = G_0(k_0 \sin \theta) \cos \theta \cdot T(\theta) \quad (12)$$

where $T(\theta)$ is the sheath transmission pattern given by

$$T(\theta) = \frac{e^{-ik_0 a \cos \theta}}{\cos [k_0 a (\epsilon_r - \sin^2 \theta)^{1/2}] - \frac{i \cos \theta}{(\epsilon_r - \sin^2 \theta)^{1/2}} \sin [k_0 a (\epsilon_r - \sin^2 \theta)^{1/2}]} \quad (13)$$

$T(\theta)$ is, of course, dependent on θ and can therefore be expected to alter, at least to some extent, the radiation pattern of the aperture for all angles. However, the most significant changes occur at angles near $\theta \simeq \pi/2$, and at frequencies in the vicinity of cut off for a TE_n surface wave on a dielectric slab covering a ground plane.² These waves begin to propagate for respective values of $k_0 a$ given by

$$(k_0 a)_n = \frac{(2n-1)\pi}{(\epsilon_r - 1)^{1/2}} \quad (14)$$

Under the conditions $\theta = \pi/2$ and $k_0 a = (k_0 a)_n$, the denominator of equation 13 vanishes, and although this behavior must be weighted by the fact that in equation 12, for $\theta \rightarrow \pi/2$, $\cos \theta \rightarrow 0$, the overall

effect is still to produce a broadening of the pattern and therefore a resonant component of radiation near the end-fire direction. Typical curves for $G(\theta)$ illustrating this effect are shown in Fig. 5 for values of $k_0 a$ centered about $(k_0 a)_1$, with $G_0(k_0 \sin \theta) \equiv 1$, $\epsilon_r = 6.0$. The results therefore pertain to the appropriate Green's function. With regard to interpretation of these curves, it should be noted that, strictly speaking, the results cannot be applied at angles arbitrarily close to 90° . This is because eventually one reaches the outer boundary of the dielectric sheath in which a different solution must be used. The curves have been drawn up to 90° under the assumption that in the far field the sheath occupies a negligibly small angular sector.

While the distortion of the radiation pattern has the physical appearance of a surface wave, in the sense that its energy is most significant near the dielectric interface, it is actually quite different in several respects. First, the radiation discussed here belongs to the continuous, rather than to the discrete spectrum of the aperture radiation field. Its amplitude thus decays inversely with distance from the

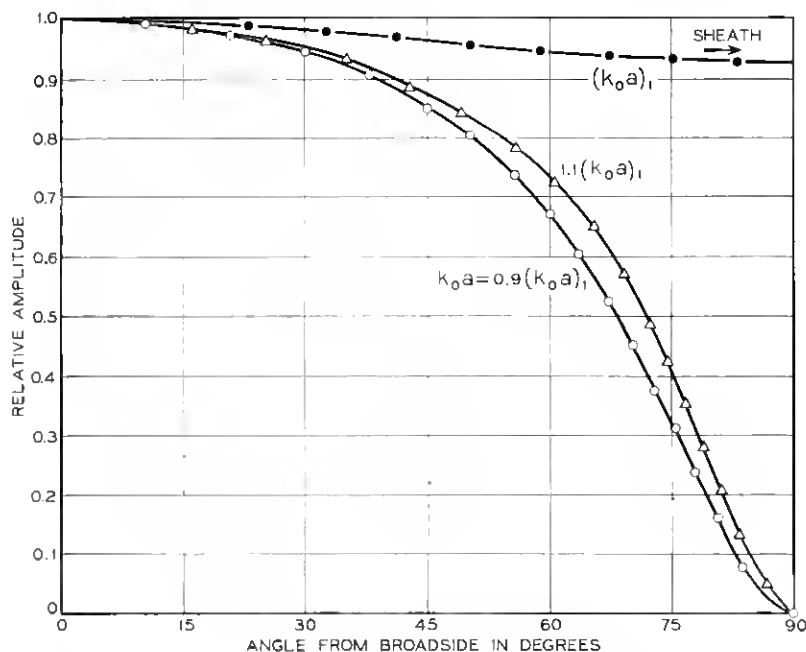


Fig. 5— $G(\theta)$ (normalized to unity at $\theta = 0^\circ$) for values of $k_0 a$ near $(k_0 a)_1$, $G_0(k_0 \sin \theta) \equiv 1$, $\epsilon_r = 6.0$.

aperture, rather than being independent of distance, as for an unattenuated mode guided by the slab-ground combination. Furthermore, the end-fire radiation does not exhibit a cutoff characteristic but instead has essentially a symmetrical amplitude variation about the frequencies given by equation 14.

The surface wave modes excited by the aperture are, on the other hand, associated with the discrete spectrum of the radiation field, and are derived mathematically from the residues of the inversion integral with respect to its poles. These poles correspond to solutions of the equation

$$\cos \beta a + \frac{\alpha_0}{\beta} \sin \beta a = 0 \quad (15)$$

where $\alpha_0 = (h_0^2 - k_0^2)^{1/2}$, h_0 being the surface wave propagation constant. There is no detailed discussion of surface wave excitation here because not enough information is yet available to accurately estimate the appropriate excitation coefficient. This observation is made, to some extent, *a posteriori*, from the fact that the "reasonable" assumption of an unperturbed TE_{10} waveguide mode seems to yield a surface wave component considerably higher than we have observed experimentally.⁴ For example, theoretical calculations reported in the literature lead to the conclusion that the surface wave extracts as much as 50 percent of the total radiated power over a wide range of frequencies. If this were generally true, the effects would be visible not only as a substantial increase in end-fire radiation but as a corresponding loss in the broadside direction. Section III shows that neither of these effects was observed in the expected manner.

A possible explanation for this discrepancy can be found in the fact that the surface wave excitation coefficient is proportional to $G_0(h_0)$, the Fourier transform of the aperture field distribution, evaluated for the surface wave propagation constant h_0 . Since we are interested in dielectric constants greater than unity, $h_0 \geq k_0$, and it is therefore appropriate to cast $G_0(h_0)$ in the form (assuming E_0 is symmetric with respect to z),

$$G_0(h_0) = \sum_{m=0}^{\infty} C_m \frac{E_0^{(m)}(z=l)}{(h_0/k_0)^{m+1}} \quad (16)$$

where the C_m are constants and $E_0^{(m)}(z=l)$ represents the m th derivative of the aperture field, evaluated at the edge.⁶ Equation (16) is different from the analogous formula for the radiation field, which would be a series in direct powers of h/k_0 in which the coefficients would

be weighted integrals of the aperture field. This dependence of surface wave excitation on conditions at the edge of the aperture makes the problem very difficult to analyze, especially since measurements have shown the field in this region to change significantly when a sheath is present.⁴ A physical interpretation would be that surface wave excitation depends on diffraction rather than direct radiation.

III. EXPERIMENTAL RESULTS

The apparatus, illustrated in Fig. 6, consists of a network feeding an open X-band (WR-90) waveguide flanged to a ground plane. So as to simulate the two-dimensional situation analyzed in the previous section, parallel conducting walls in the H-plane were used, as shown in Fig. 7. With this configuration, no additional field components are induced (at least theoretically), and the fields are essentially independent of position in the E-plane. The ground plane and aperture were covered by a uniform slab of stycast material with dielectric constant of 6.0 and thickness such that the $(TE)_1$ mode cut-off frequency was 10.0 GHz.

The measurements determined the individual signals received by the end-fire and broadside detectors, which consisted of open-ended waveguides terminated with broadband matched crystals. These were

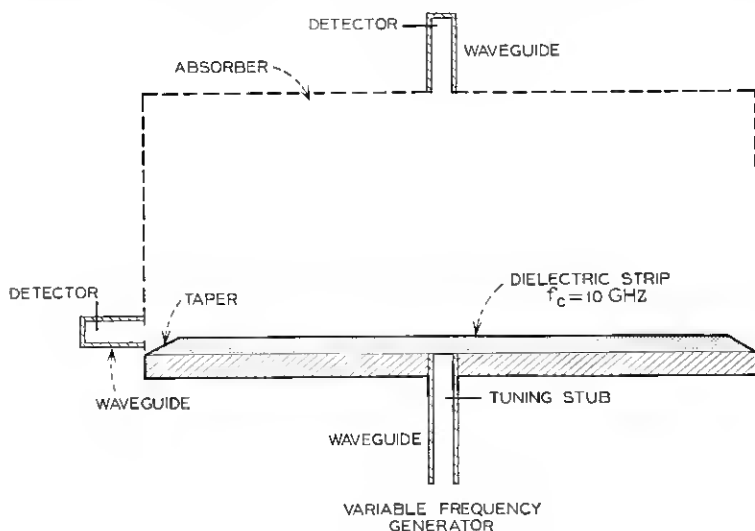


Fig. 6 — Apparatus for measuring broadside and end-fire radiation.

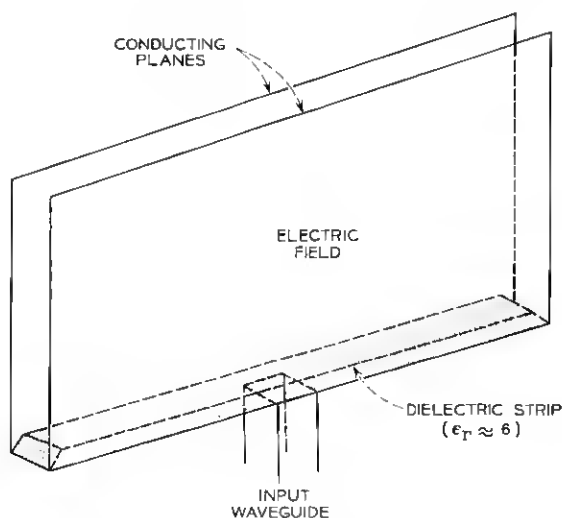


Fig. 7 — Use of parallel conducting planes to simulate two-dimensional geometry.

compared with the power incident on the aperture by a ratio meter having one terminal connected to the input waveguide via a directional coupler. At each frequency the tuning stub was adjusted to keep the return loss below -30 dB; the results therefore pertain to a matched element.

In order to avoid mutual coupling between waveguide detectors, respective measurements of broadside and end-fire signals were made with the other detector removed. Since the waveguides were mounted in brackets which could be rigidly connected to the conducting planes, repeatability was not considered to be a serious problem.

Figure 8 shows the experimental results, which demonstrate the resonant end-fire radiation phenomenon. The peak of the end-fire signal occurs at 10.0 GHz, as expected, and the general shape of the curve, down to approximately 6 dB below the peak value (normalized to 0 dB maximum), accurately follows the theoretical behavior. The latter was determined by calculating $\cos \theta T(\theta)$ for a value of $\theta = 88^\circ$. In this regard, it was found by direct calculation that the shape of the relative variation with frequency is not sensitive to small deviations from 90° . The result given in Fig. 8 should therefore be a reasonable estimate for the behavior of the waveguide aperture receiver. Notice that 0 dB is defined as the measured end-fire signal

at 10 GHz and that the theoretical curve is also normalized at this frequency. Thus no attempt has been made to arrive at an absolute corroboration, which would require both the solution inside the dielectric slab and a detailed description of radiation at the end taper. The deviations in the end-fire radiation in Fig. 8 below 6 dB probably result from these latter aspects.

Under matched conditions, conservation of energy requires that an increase in radiation in any direction must be accompanied by a corresponding reduction in other directions. This is clearly evidenced by the decrease in broadside radiation in the vicinity of 10.0 GHz. The reduction amounts to approximately 3–4 dB, which is quite significant, perhaps even more so in terms of antenna performance than the increase in the end-fire signal. The displacement of the minimal frequency to the slightly lower value of 9.7 GHz is, in all likelihood, caused by the generally increasing nature of the broadside signal before the dip occurs, attributed to the slow increasing gain

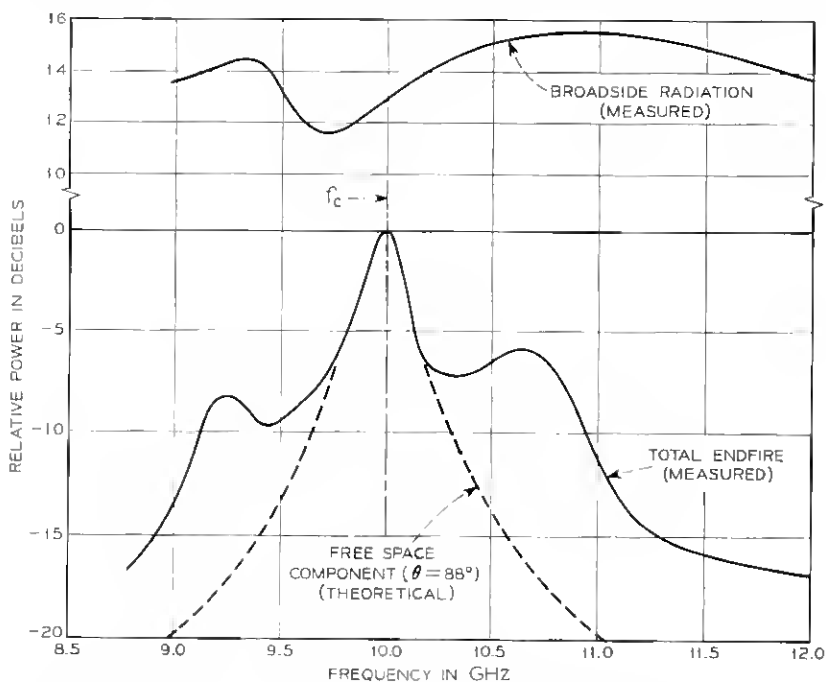


Fig. 8—Observed end-fire and broadside radiation under matched conditions.

of the receiving aperture with frequency. This would tend to skew the curve slightly to the left.*

In interpreting these experimental results, it is worth noting that strong coupling to a surface wave in this experiment would be seen in two ways. First, the end-fire radiation would exhibit a cut-off characteristic in which the amplitude would be relatively low below the cut-off frequency, in this case 10.0 GHz, at which point it would increase to a higher value. Second, at approximately the same frequency the broadside radiation would correspondingly decrease. Since the experimental results do not behave in this way, but rather in a manner predictable by a far field analysis, it is concluded that strong coupling to the surface wave component did not occur for this particular set of parameters.

IV. SUMMARY AND CONCLUSIONS

The purpose of this study has been to examine, both theoretically and experimentally, the radiating characteristics of an aperture-type antenna covered by a dielectric sheath. Such an antenna might represent, for example, an element of a phased array which has been protected against a high temperature environment.

The first principal effect of the sheath on the pattern of a matched element is to introduce a broadening of the radiation pattern and a resulting component of radiation in the end-fire direction at frequencies near the cut-off frequency of a surface wave on the dielectric slab. However, it is important to distinguish this phenomenon, which is properly viewed as a distortion of the far-zone radiation pattern, from what is commonly referred to as a surface wave, which is a separate mode of propagation belonging to the discrete spectrum of the radiation field. No effects attributable to the latter were observed in the experiment, showing that the excitation was negligibly small over the measured frequency range.

Under matched conditions, there must be a corresponding dip in the broadside radiation over the same frequency range. This requirement follows directly from energy conservation.

It is concluded that a matched phased array element is not sufficient to guarantee that the antenna is functioning as required. Dielectrics can have a pronounced effect on the directivity and efficiency

* Recent computational studies by C. P. Wu corroborate this slight frequency shift of the dip in broadside radiation.

of aperture radiators, especially near frequencies which are characteristic of surface wave propagation along some part of the structure.

V. ACKNOWLEDGMENT

The author would like to thank Mr. P. J. Puglis, who actively contributed to all aspects of this work. Conversations with Dr. C. P. Wu were also most helpful.

REFERENCES

1. Galindo, V., and Wu, C. P., "Dielectric Loaded and Covered Rectangular Waveguide Phased Arrays," B.S.T.J., 47, No. 1 (January 1968), pp. 93-116.
2. Collin, R. E., *Field Theory of Guided Waves*, New York: McGraw-Hill, 1960, p. 470.
3. Mathews, J., and Walker, R. L., *Mathematical Methods of Physics*, New York: W. A. Benjamin, 1964, p. 78.
4. Crowell, W. F., Rudduck, R. C., and Hatcher, D. M., "The Admittance of a Rectangular Waveguide Radiating into a Dielectric Slab," IEEE Trans. Antennas and Propagation, AP-15 (September 1967), pp. 627-633.
5. Erdélyi, A., *Asymptotic Expansions*, New York: Dover Publications, 1965, p. 46.

